Analysis of Tropical Cyclogenesis in the Western North Pacific for 2000 and 2001*

BING FU

Department of Meteorology, University of Hawaii at Manoa, Honolulu, Hawaii

TIM LI

International Pacific Research Center, and Department of Meteorology, University of Hawaii at Manoa, Honolulu, Hawaii

MELINDA S. PENG

Marine Meteorology Division, Naval Research Laboratory, Monterey, California

FUZHONG WENG

NOAA/NESDIS/Office of Research and Applications, Camp Springs, Maryland

(Manuscript received 13 March 2006, in final form 1 November 2006)

ABSTRACT

High-resolution satellite data and NCEP–NCAR reanalysis data are used to analyze 34 tropical cyclone (TC) genesis events in the western North Pacific during the 2000 and 2001 typhoon seasons. Three types of synoptic-scale disturbances are identified in the pregenesis stages. They are tropical cyclone energy dispersions (TCEDs), synoptic wave trains (SWTs) unrelated to preexisting TCs, and easterly waves (EWs). Among the total 34 TC genesis cases, 6 are associated with TCEDs, 11 cases are associated with SWTs, and 7 cases are associated with EWs. The analyses presented herein indicate that the occurrence of a TCED depends on the TC intensity and the background flow, with stronger cyclones and weaker background easterlies being more likely to induce a Rossby wave train. Not all Rossby wave trains would lead to the formation of a new TC. Among the 11 SWT cases, 4 cases are triggered by equatorial mixed Rossby–gravity waves. Cyclogenesis events associated with EWs are identified by the westward propagation of the perturbation kinetic energy and precipitation fields. For all three types of prestorm disturbances, it seems that scale contraction of the disturbances and convergence forcing from the large-scale environmental flow are possible mechanisms leading to the genesis. Further examination of the remaining 10 genesis cases with no significant prior synoptic-scale surface signals suggests three additional possible genesis scenarios: 1) a disturbance with upper-tropospheric forcing, 2) interaction of a preexisting TC with southwesterly monsoon flows, and 3) preexisting convective activity with no significant initial low-level vorticity. Tropical intraseasonal oscillations have a significant modulation on TC formation, especially in 2000.

1. Introduction

Tropical cyclone (TC) genesis is a process through which a tropical disturbance rapidly develops into a warm-core, cyclonic system with sustainable winds. Due to the lack of reliable data over open oceans and the complicated interactions involved, our understanding of TC genesis remains very limited. Recent advances in satellite-retrieval products make it possible to explore more detailed atmospheric processes and circulation patterns associated with tropical cyclogenesis. In this study, we examine synoptic-scale disturbances prior to the formation of TCs in the western North Pacific (WNP) based on satellite observations and National Centers for Environmental Prediction–National Center for Atmospheric Research (NCEP–NCAR) reanalysis fields.

The WNP is the most active region for TC genesis.

* School of Ocean and Earth Science and Technology Contribution Number 7067 and International Pacific Research Center Contribution Number 440.

Corresponding author address: Bing Fu, Dept. of Meteorology, University of Hawaii at Manoa, 2525 Correa Rd., Honolulu, HI 96822.
E-mail: bingf@hawaii.edu

DOI: 10.1175/WAF1013.1

The summer mean low-level circulation in the WNP is characterized by a zonal confluence zone between the monsoon westerlies and the easterly trade winds, and a meridional shear line along 5°N, 150°E, and 20°N, 120°E at 850 hPa separating the westerlies to the south and the easterlies to the north. The low-level convergence leads to strong upward motion and intense cumulus convection. That region overlaps with the monsoon trough, with positive low-level vorticity and relatively weak vertical wind shear. Ritchie and Holland (1999) summarized three environmental flow regimes that favor cyclogenesis in the WNP. These are the monsoon shear line, the monsoon confluence zone, and the monsoon gyre. While these large-scale flow patterns provide ideal background stages for tropical cyclone genesis, the synoptic-scale waves/disturbances (and/or embedded mesoscale convective systems) actually lead to the formation of individual storm events. Thus, the timing of TC formation depends crucially on the evolution of the synoptic waves/disturbances and their interactions with large-scale background flow.

The first type synoptic-scale disturbance associated with TC genesis in the WNP is Rossby wave energy dispersion from a preexisting TC (TCED hereafter). An intense TC is subject to Rossby wave energy dispersion. While it moves northwestward due to mean flow steering and the planetary vorticity gradient, Rossby waves emit energy southeastward (Anthes 1982; Flierl 1984; Flierl and Haines 1994; Luo 1994; McDonald 1998). As a result, a synoptic-scale wave train with alternating anticyclonic and cyclonic vorticity perturbations forms in its wake (Carr and Elsberry 1994, 1995). This TC genesis associated with TCEDs has been suggested previously (e.g., Frank 1982; Davidson and Hendon 1989; Briegel and Frank 1997; Ritchie and Holland 1997) without detailed descriptions of the wave trains and their evolutions. Recently, using satellite products and model simulations, Li et al. (2003) and Li and Fu (2006) demonstrated the generation of a Rossby wave train in the wake of a TC and the formation of a new cyclone.

The second type of disturbance in the pregenesis stage is a synoptic-scale wave train (SWT) that is not related to the energy dispersion of a preexisting TC. The SWT is oriented in a northwest–southeast pattern and is often observed during the summertime in the WNP. Lau and Lau (1990) first identified this type of wavelike disturbance by analyzing the observed low-level vorticity and meridional wind fields. The wave train generally propagates northwestward and has a wavelength in the range of 2500–3000 km and a period of 6–10 days. Chang et al. (1996) found that the majority of the TC centers collocate with the cyclonic vorticity region of the wave train, suggesting a possible role for the wave train in the triggering TC formation. Dickinson and Molinari (2002) attributed the generation of SWTs to the development of equatorial mixed Rossby–gravity (MRG) waves located initially near the equator and later tilted northwestward and transitioned into an off-equatorial disturbance. Three TCs formed on the cyclonic gyres of the transformed SWT in their study.

The third type of synoptic-scale perturbation that may induce cyclogenesis in the WNP is the easterly wave (EW). One of the earliest discussions of TC genesis associated with easterly waves was presented by Riehl (1948), who investigated a typical cyclogenesis case in the WNP and suggested that the genesis can occur when the low-level cyclone within a wave becomes collocated with an upper-level ridge so that the upper-level outflow from the storm is enhanced by the pressure distribution of the ridge. Yanai (1961) conducted a detailed analysis of Typhoon Doris (1958) and proposed three development stages for the typhoon formation, including an initial stage of an EW with a cold core, a transition to a warm-core stage, and a rapid development stage. The role of EWs in TC formation in the western Pacific was also documented in several later papers (Yanai et al. 1968; Chang et al. 1970; Reed and Recker 1971). Kuo et al. (2001) demonstrated, using a barotropic model, that the scale contraction of EWs could lead to the accumulation of kinetic energy at a critical longitude where the monsoon westerly meets the trade easterly. This energy accumulation mechanism may lead to the successive development of synoptic-scale disturbances at the critical longitude. This mechanism is parallel to those previously used to explain Atlantic tropical cyclogenesis from EWs by Shapiro (1977) and energy accumulation and emanation in the upper troposphere by Webster and Chang (1988).

All three of the precyclogenesis disturbances discussed are most prominent in low-level atmospheric circulations. Thus, one may take advantage of Quick Scatterometer (QuikSCAT) satellite products to explore their structures and the characteristics of their evolutions prior to tropical cyclogenesis. In addition, other satellite products and reanalysis fields will also be used to examine convection and other possible upper-tropospheric forcings. This paper is organized as follows. The data and methods used are described in section 2. The TC formations associated with different genesis processes are discussed in section 3. In section 4, the impact of the atmospheric intraseasonal oscillation on TC genesis is examined. A summary and discussion are given in section 5.

2. Data and analysis methods

a. Data

The primary data used in this study are from the Tropical Rainfall Measuring Mission (TRMM) Microwave Imager (TMI) and QuikSCAT wind retrievals. The TMI data are retrieved by a radiometer on board the TRMM satellite, launched on 27 November 1997. TRMM is a joint mission supported by National Aeronautics and Space Administration and the National Space Development Agency of Japan. TMI data cover the entire global tropical region between 40°S and 40°N. It provides 10-m surface wind speed (11 and 37 GHz), sea surface temperature, atmospheric water vapor, cloud liquid water, and precipitation rate with a horizontal resolution of 0.25° × 0.25°. The data used in this study are the 3-day-average wind speed, cloud liquid water, and the precipitation rate from the 11-GHz channel. We made some comparisons between the wind speed retrieved from the 37- and the 11-GHz channels, and our results show there is little difference between them. The QuikSCAT data are retrieved by a microwave scatterometer termed SeaWinds on board the *QuikBird* satellite launched in June 1999. The primary mission of QuikSCAT is to measure winds near the sea surface. By detecting the sea surface roughness, QuikSCAT uses an empirical relationship to calculate the 10-m surface wind speed and direction. The products from this scatterometer include 10-m surface zonal and meridional wind speeds at a daily interval. The QuikSCAT data cover the global oceans, with a horizontal resolution of 0.25° × 0.25°. Linear optimal interpolation is used to fill in missing data over the open ocean.

In addition, we use the NCEP–NCAR reanalysis and outgoing longwave radiation (OLR) data from National Oceanic and Atmospheric Administration–Cooperative Institute for Research in Environmental Sciences. Both data have a horizontal resolution of 2.5° × 2.5°. The purpose of using the NCEP–NCAR reanalysis is twofold. First, note that neither the TMI nor QuikSCAT data cover land. Although we are focusing on oceanic regions, the data need to be continuous for our analysis procedure. Thus, we use the NCEP–NCAR data to fill in all the land areas. Second, the NCEP–NCAR reanalysis is used to obtain the vertical structures of synoptic-scale flow systems associated with cyclogenesis processes, as neither the TMI nor QuikSCAT data provide upper-level atmospheric information. However, the strength of the synoptic perturbations may often be underestimated due to its coarse resolution. Global daily OLR data are further used to study the modulation of TC genesis by low-frequency climate variabilities. The TC best-track data used in this study originated from the TC advisory issued by the Joint Typhoon Warning Center (JTWC). The TC minimum pressure data are from the Hong Kong Observatory.

b. Analysis methods

To examine the synoptic-scale atmospheric signatures prior to TC formation, a time-filtering method is used to obtain 3–8-day disturbances for both the QuikSCAT and TMI data. The selection of such a 3–8-day bandwidth is based on the results of Lau and Lau (1990, 1992), who pointed out that the most significant synoptic-scale wave spectrum appears in this band in the WNP. The filtering scheme used in this study is originally from Murakami (1979) for studies of large-scale deep convection. The response function for this filter is a Gaussian function. In this 3–8-day bandwidth, the strongest response is around 5 days, with a maximum response of 1.0. The same filtering with a 20–70-day bandwidth is later applied to the data to study the modulation of the intraseasonal oscillation (ISO) on TC genesis. Within that bandwidth, the strongest response occurs around 42 days. In addition, a low-pass filter with a period greater than 20 days is used to obtain the large-scale background circulation patterns associated with cyclogenesis.

Different cyclogenesis scenarios will be identified based on the following synoptic analysis approach. First, we identify TC formations associated with TCEDs. If a new TC formed in the cyclonic circulation embedded within the wave train produced by a preexisting TC, this new TC belongs to the TCED category. If a new TC formed within a synoptic wave train that did not involve a preexisting TC, it belongs to the SWT group. For the remaining cases, we examine the time–longitude map of the 3–8-day filtered kinetic energy and precipitation rate along the latitude where a new TC formed. A TC formation belongs to the EW group when the genesis is embedded within the westward propagation of both the perturbation energy and precipitation fields. The reason for classifying the cases in this order is that most of the wave trains themselves (either produced by TCEDs or other mechanisms) usually move westward as well. We categorize the ones with both north and west movements as being in the SWT group first, to distinguish them from those formed within EWs. We speculate that some of previous studies may have overestimated the occurrence of TC genesis under EW conditions.

TABLE 1. Classifications of the 34 TCs in 2000 and 2001.

Genesis scenarios	2000	2001
TCEDs	Ewiniar, Prapiroon, Sonamu	Utor, Trami, Toraji
SWTs	Kirogi, Tembin, Bolaven, Bilis, Wukong, Bopha	Chebi, Durian, Man-yi, Pabuk, Sepat
EWs	Chanchu, Jelawat, Shanshan	Kong-rey, Wutip, Danas, Francisco
Other scenarios	Kai-tak, Kaemi, Maria, Saomai	Yutu, Usagi, Fitow, Nari, Vipa, Lekima

3. Tropical cyclogenesis in the WNP in 2000 and 2001

Thirty-four tropical cyclogenesis events were identified in the WNP during the boreal summer seasons of 2000 and 2001. Table 1 list all TCs and the characteristics of their pregenesis disturbances based on our categories. Among the 34 TCs, 6 (18%) are associated with TCEDs, 11 cases (32%) are associated with SWTs and 7 cases (21%) are associated with EWs. In the following we describe each of these scenarios and present an example for each type.

a. TCED

1) ROSSBY WAVE TRAIN BEHIND TROPICAL CYCLONES

The first type of TC genesis is associated with the Rossby wave energy dispersion of a preexisting TC. Detailed descriptions of the wave train patterns and their evolving characteristics are given in Li and Fu (2006).

An example, a TC formation following Typhoon Utor (formed on 1 July 2001), is discussed here. During the first 2 days after the formation of Utor, there was little signal of a wave train along its wake while its strength was still very weak. The estimated minimum sea level pressure (MSLP) from the JTWC was around 1000 hPa. As Utor moved northwestward, it rapidly intensified. By 3 July 2001, the MSLP dropped to 976 hPa and a Rossby wave train formed at its wake. Figure 1 contains the time evolution of the 3–8-day filtered surface synoptic-scale wind fields near Utor from the QuikSCAT data and it shows the temporal evolution of the Rossby wave train. By 5 July 2001, the wave train was orientated in a northwest–southeast direction with a wavelength of about 2500 km. Characteristics similar to TC dispersive waves were also observed by Li et al. (2003).

The development of the Rossby wave train associated with Typhoon Utor eventually leads to the formation of a new TC, Trami, on 9 July 2001 in the positive vorticity center with the scale contraction of the Rossby wave between 7 and 9 July.

The vertical variation of the wave train produced by the energy dispersion from Utor can be observed in the horizontal wind fields of the 3–8-day filtered NCEP–NCAR reanalysis data at different levels (Fig. 2). There is no clear wave pattern at 200 hPa, but the wave train is evident at 500 hPa and at lower levels with little vertical tilt. At the surface, the cyclonic circulation of the wave train coincides with the region of concentrated cloud liquid water whereas the anticyclonic regions are cloud free (Fig. 2d).

2) FACTORS CONTROLLING WAVE TRAIN DEVELOPMENT AND CYCLOGENESIS

Our analyses indicate that not all TCs have a Rossby wave train in their wakes. A question arises as to what determines the formation of the Rossby wave train. Factors that affect TC Rossby wave energy dispersion have been studied previously within theoretical frameworks. For example, Flierl et al. (1983) proposed that the relative angular momentum (RAM) and the horizontal scale of a TC play important roles in determining the wave energy dispersion. Shapiro and Ooyama (1990) showed, with numerical simulations, that there is no Rossby wave energy dispersion for an initial vortex with zero RAM.

Because detailed information on the structure of TCs is unavailable over open oceans, we explore and seek relationships between the occurrences of wave trains and TC intensities and background wind fields. A total of 233 snapshots for the 34 TCs are examined. Table 2 shows how the occurrence of the wave train depends on TC intensity. For our limited cases, 86.7% of the strong TC snapshots with an MSLP lower than 960 hPa formed a Rossby wave train in their wakes. While for weaker TC snapshots (MSLP greater than 980 hPa), only 30.6% formed a Rossby wave train. We further investigated the characteristics of strong TC snapshots that do not have a Rossby wave train and found that they all were located east of 150°E where strong easterly trade winds are dominant. Therefore, our analyses suggest that the existence of Rossby wave trains depends on both the TC intensity and the background wind. A weak cyclone can induce only weak dispersive waves and we speculate that a strong background wind would generate larger shear and convergence/

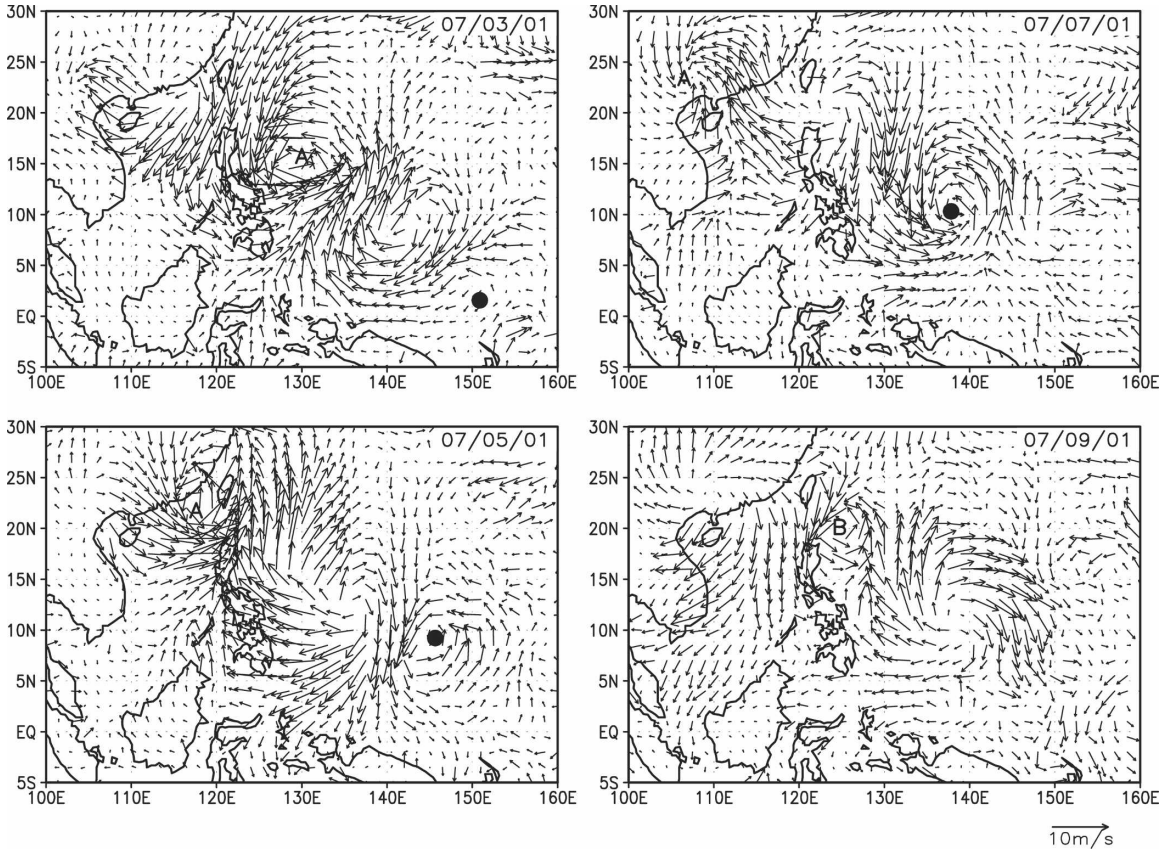

FIG. 1. The 3–8-day filtered QuikSCAT surface wind data showing the time evolution of a Rossby wave train associated with the energy dispersion of TC Utor. The letter A represents the center location of Utor, which formed on 1 Jul 2001. The letter B represents the center location of a new TC named Trami, which was generated on 9 Jul 2001 in the wake of the Rossby wave train of Utor. The dots represent the centers of cyclonic circulation prior to genesis of TC Trami.

divergence that would break or interfere with a weak Rossby wave train.

Previous studies showed that energy dispersion is related to both the intensity and the size of the original vortex in a nondivergent barotropic model (Carr and Elsberry 1995). It is difficult to obtain reliable TC size/structure data; thus, we could not provide robust results to demonstrate the relationship between TC size/structure and Rossby wave train. We will examine this in the future.

Not all TC-induced Rossby wave trains led to new cyclogenesis. Among all of the 34 cases we studied, 17 of the 23 cases that induced Rossby wave trains did not lead to cyclogenesis, while only 6 of 23 cases resulted in a new TC. This raises another question, namely, what factors determine the likelihood of cyclogenesis in the wave train? We hypothesize that whether a Rossby wave train can develop into a new TC depends on the background flow within which the wave train is embedded. To identify the difference between the background flows of the developing and nondeveloping TC dispersion wave trains, we investigated the large-scale variability by applying a low-pass filter with periods of greater than 20 days to all the variables. Composites were centered on developing and nondeveloping cyclonic circulations in the wave train. For the developing cases, the day immediately before a TC formation was selected as the centered time. For the nondeveloping cases, we chose the strongest cyclonic circulation from the wave train behind a TC. Figure 3 shows some of the large-scale variables averaged in a $5° \times 5°$ box centered at the cyclonic vorticity center of the wave train. There are clear differences between the developing and nondeveloping cases as is revealed by the large-scale (note that the data have been filtered to retain features with periods greater than 20 days) low-level vorticity, divergence, moisture conditions, and vertical wind shears. The low-level convergence and vorticity show a significant difference between the developing cases and the nondeveloping cases. The developing cases have larger positive vorticity and larger convergence, which is a situation that is favorable for TC genesis. The 3 m s^{-1}

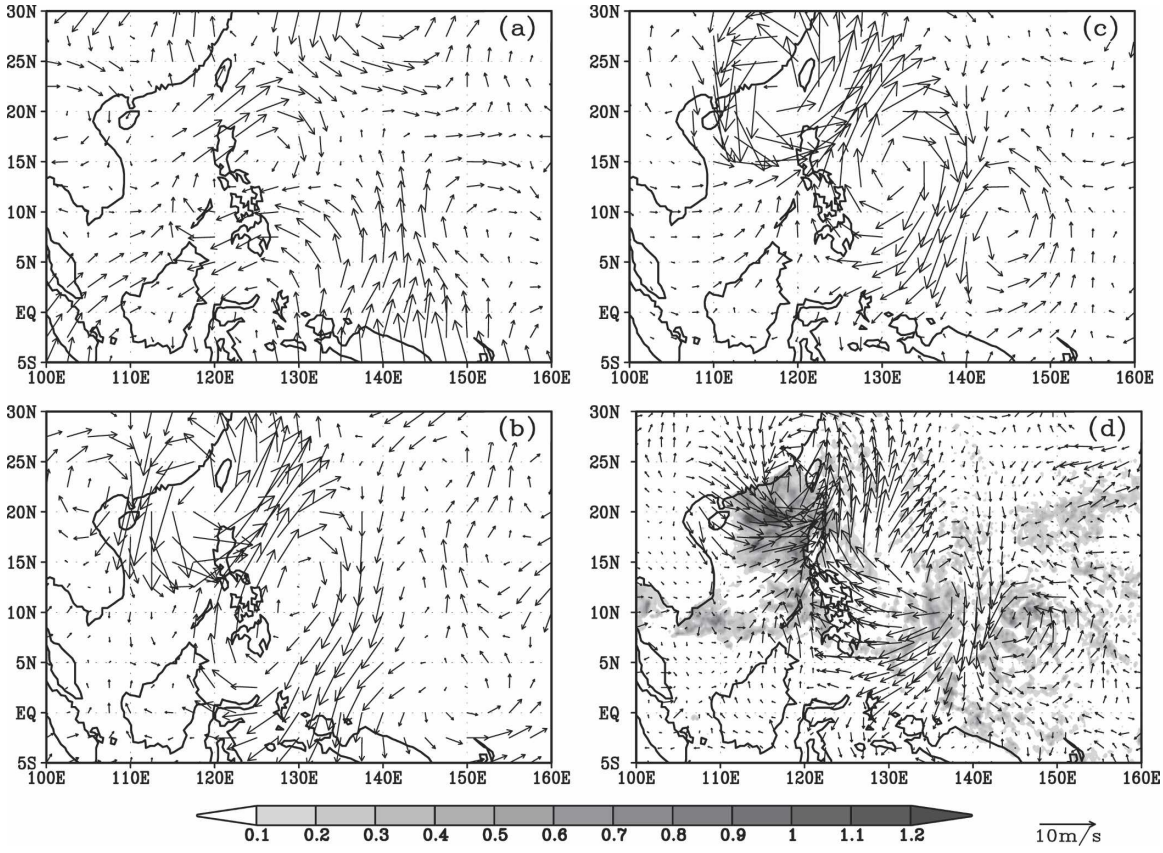

FIG. 2. Horizontal structure of the wave train produced by a TCED from Typhoon Utor on 5 Jul 2001. The wind fields are 3–8-day filtered NCEP–NCAR reanalysis data at (a) 200, (b) 500, and (c) 850 hPa. (d) The 3–8-day filtered QuikSCAT surface wind and TMI cloud liquid water data (shading; mm).

vertical shear difference in the background winds between the developing cases and the nondeveloping cases may be the most important factor among the results of comparisons for all these four large-scale variables. The relative humidity also indicates a favorable environmental condition for TC genesis in the developing cases, although the difference is small. All these aspects are consistent with the general understanding of environments that are favorable for TC genesis (Gray 1968, 1975; McBride and Zehr 1981).

A composite of the TMI cloud liquid water data also shows differences between the developing and nondeveloping cases (Fig. 4). The nondeveloping cases have smaller liquid water amounts and the developing cases have larger amounts in an annulus around the storm center. This ringlike feature may be the preferred location of active deep convection and of the formation of the eyewall in the development of the storms.

TABLE 2. Percentage of individual cases with a wave train for the different MSLP categories.

	MSLP < 960 hPa	960 hPa ≤ MSLP ≤ 980 hPa	MSLP > 980 hPa
Percentage	86.7	39.2	30.6

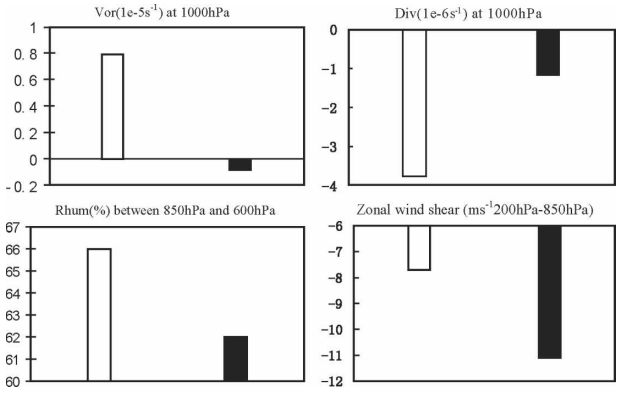

FIG. 3. Composites of NCEP–NCAR reanalysis 20-day low-pass-filtered vorticity, divergence, and relative humidity averaged between 850 and 600 hPa, and zonal wind shear (200–850 hPa) for developing cases (white bars) and nondeveloping cases (black bars) in the Rossby wave trains.

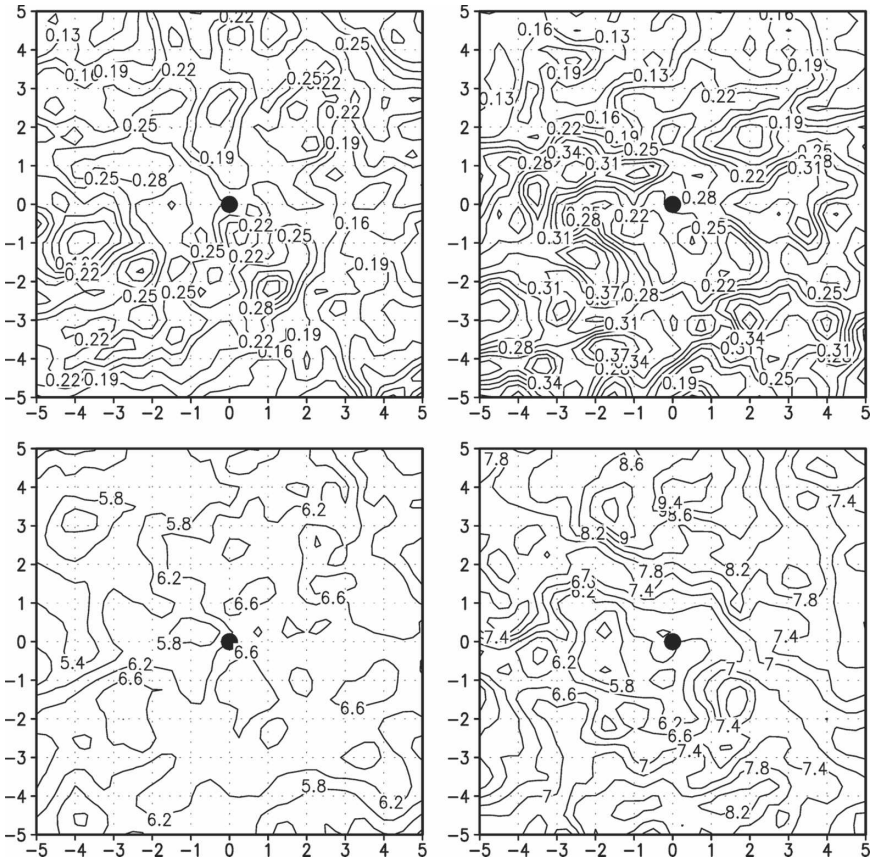

FIG. 4. TMI (top) cloud liquid water (mm) and (bottom) surface wind speed composites for (left) nine nondeveloping and (right) six developing cases. The dot represents the circulation center. The unit of the horizontal (vertical) axis is degrees longitude (latitude).

b. TC genesis in an SWT

The second type of TC genesis is through the development of an SWT that does not involve a preexisting TC. A northwest–southeast-oriented wave train is often observed in 3–8-day filtered wind fields in the WNP (Lau and Lau 1990, 1992). This type of wave train has a dominant wavelength of about 2000–2500 km and propagates northwestward. The intensities of the wave trains increase as they move northwestward from the lower latitudes to the WNP. The origin of the SWT is suggested by Li (2006) to be a result of the instability of the summer mean flow in the Tropics with a convection–circulation feedback mechanism. The initial triggering of this instability may sometimes be traced back to equatorial MRGs, implying an equatorial to off-equatorial transition of wave perturbations.

Our QuikSCAT data analysis shows that during the 2000 and 2001 typhoon seasons, there were 11 TCs that formed in the SWT. An example is illustrated here for the formation of Typhoon Man-yi, which formed on 2 August 2001 (Fig. 5). Three days prior to its genesis, a northwest–southeast-oriented wave train developed in the WNP (on 30 July 2001). This wave train had well-defined cyclonic and anticyclonic circulations, and covered a region between 0°–25°N and 130°–160°E. The wave train moved northwestward slowly. On 2 August, Man-yi developed in the cyclonic vorticity region of the wave train.

Figure 6 shows this SWT at different levels, as retrieved from the NCEP–NCAR reanalysis fields on 31 July, that eventually led to the formation of Typhoon Man-yi. At 850 hPa (Fig. 6c), the wave train has a rather long north–south scale, making its northwest–southeast orientation less apparent. At 500 hPa, the wave train appears to be more east–west oriented with two cyclonic circulations along 163°E. At 200 hPa, the wave train is east–west oriented. The variation of the wave train in the vertical deserves more study and is beyond the scope of the present study. The cloud liquid water distribution in this case is not as organized as that induced by TCEDs. We have plotted the vertical profile along the axis of this wave train and note that, in general, most of the vertical profiles of the SWT cases show

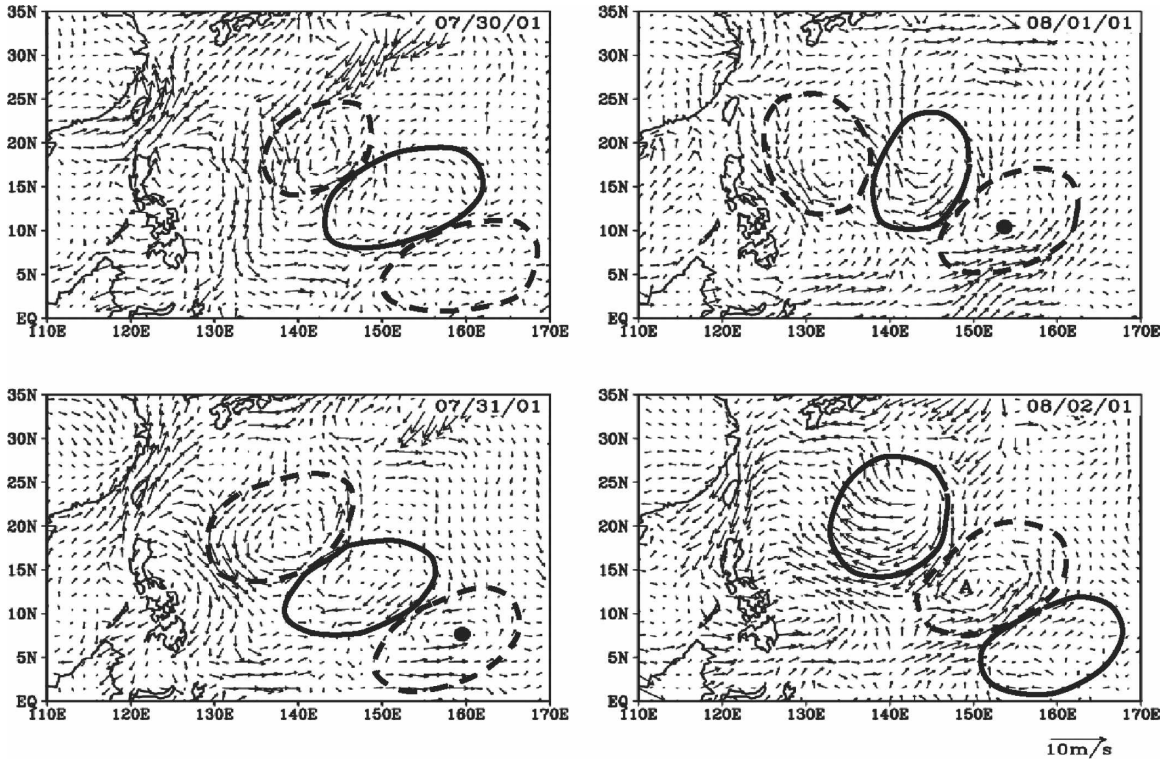

FIG. 5. Time evolution of 3–8-day filtered QuikSCAT surface wind patterns associated with the synoptic wave train. The dots indicate the center location of the cyclonic circulation prior to the genesis of Typhoon Man-yi; here, the letter A indicates the center location of Typhoon Man-yi on the day of genesis. Cyclonic (anticyclonic) circulation is marked with a dashed (solid) circle.

a less coherent dynamic structure and weaker strength as compared with the TCED cases (figure not shown).

Among the 11 SWT cases, 4 cases are triggered by equatorial MRG waves. The basic feature of the MRG wave is an equatorially antisymmetric structure with pronounced clockwise cross-equatorial flows. An example is given in Fig. 7 for Typhoon Sepat. Note that an equatorial MRG wave appeared on 24 August 2001 near the date line. As its phase propagated westward, the group velocity of the MRG wave was eastward. This led to the development of the second MRG wave to its east, which had counterclockwise flows (the center is denoted by the letter B). Meanwhile, an anticyclonic circulation developed north of the equator (between the equator and 15°N) within the original MRG wave gyre (the center is denoted by an A). As a result, a northwest–southeast-oriented wave train developed in the WNP and was clearly seen in the wind field of 26 August. As the wave train continued to develop, a new TC named Sepat formed in the cyclonic vorticity region of the wave train on 27 August. This process has been referred to as a transition of MRG waves to off-equatorial (tropical depression) TD-type disturbances in previous studies (Takayabu and Nitta 1993; Dickinson and Molinari 2002). The energy dispersion from the previous intensified disturbance and scale contraction due to monsoon background flows may also contribute to the conversion of the TD-type disturbance.

c. TC genesis associated with EWs

Cyclogenesis associated with EWs is identified in both the perturbation kinetic energy and the precipitation fields prior to TC formation. Only cases with clear westward propagation signals in both the perturbation kinetic energy and the rainfall field are identified as the EW forcing cases.

An example of the TC formation within an EW is given for Typhoon Kong-rey, which formed on 22 July 2001. Figure 8 shows the time–longitude cross section of the perturbation energy and precipitation rate along 25°N where Kong-rey formed. Both the precipitation and the perturbation energy show clear westward propagation prior to the genesis of Kong-rey. The wave signals can be traced back 4–5 days prior to Kong-rey's formation. The EWs, as represented by both the rainfall rate and energy perturbations, show westward propagation. Note that the speeds of the waves represented by the rainfall rate and the perturbation energy are not identical, as they represent different scales in our rather wide range of the frequency band from 3 to

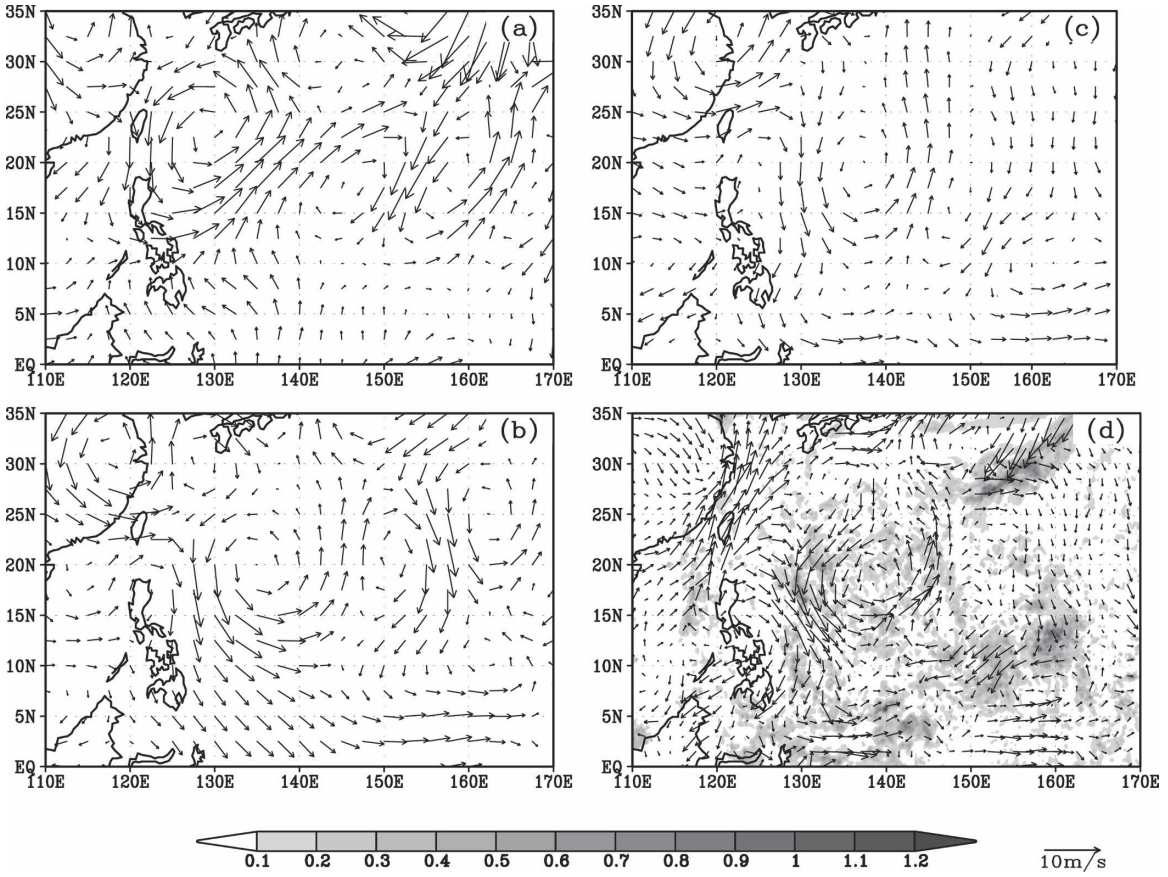

FIG. 6. Horizontal structure of the observed synoptic wave train on 31 Jul 2001. The wind fields are 3–8-day filtered NCEP–NCAR reanalysis data at (a) 200, (b) 500, and (c) 850 hPa. (d) The 3–8-day filtered QuikSCAT surface wind and TMI cloud liquid water data (shading; mm).

8 days. In addition, a time–longitude profile of the perturbation precipitation rate shows a phase speed change near 157°E with the propagation speed being faster to the east of 157°E than to the west. An approximate estimation of the phase speed would be around 4°–5° longitude per day. It was demonstrated by Kuo et al. (2001) that the scale contraction would increase the zonal wavenumber and thus slow down the wave propagation speed near the critical longitude. Because of this nonlinear process, wave energy and enstrophy can be accumulated in this area. It is different from previous linear energy accumulation theories that suggested the accumulation is accomplished by the slow down of the Doppler-shifted group velocity through the convergence of mean zonal advection.

The EW patterns at different levels are shown by the 3–8-day filtered NCEP–NCAR reanalysis fields on 18 July 2001 (Fig. 9), 4 days prior to the genesis of Typhoon Kong-rey on 22 July 2001. The analysis shows that this EW is a very deep system. It is interesting that this EW shows a clear wave train pattern at 200 hPa. This wave train pattern should be associated with Rossby wave propagation. This system is the incubator of Typhoon Kong-rey, which formed 4 days later. Figure 10 shows the vertical cross section of this EW. We can see the wave amplitude has two maxima: one is near 600–700 hPa and another is between 200 and 300 hPa. This profile is consistent with previous observational studies of EW structures (Reed and Recker 1971; Reed et al. 1977).

d. Other possible mechanisms

For the remaining 10 cases that do not have significant surface signals prior to genesis, we examine other tropospheric signals and preexisting convective activities using the NCEP–NCAR reanalysis and TMI products in order to explore other possible formation mechanisms.

1) UPPER-LEVEL TROUGH FORCING

Most of the previous studies on TC genesis associated with upper-tropospheric forcing are focused on the

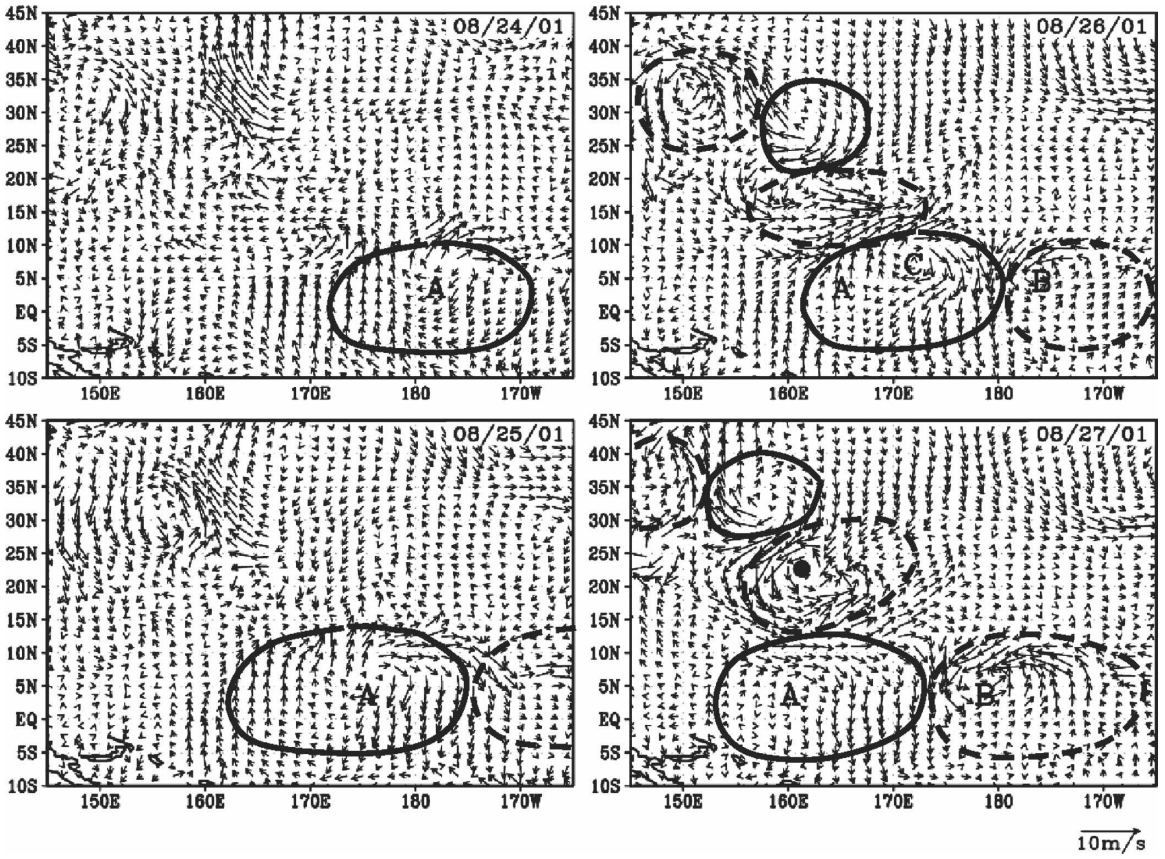

FIG. 7. Time evolution of a synoptic-scale wave train prior to the formation of Typhoon Sepat. The wind fields are 3–8-day filtered QuikSCAT surface wind. The letter A represents the center location of an original MRG wave, the letter B represents the center location of a newly developed MRG wave, and the letter C denotes the center of an anticyclonic circulation developed within the original MRG wave. A solid dot denotes the center location of TC Sepat, which formed on 27 Aug 2001. Cyclonic (anticyclonic) circulation is marked with a dashed (solid) circle.

tropical upper-tropospheric trough (TUTT). Colon and Nightingale (1963) examined the evolution of 200-hPa flows above the low-level disturbances. They found that a poleward flow aloft, such as on the eastern side of troughs in the westerlies and tropical upper-level cold lows or on the western side of anticyclones, is a favorable environmental condition for the development of low-level perturbations. Sadler (1976) developed a synoptic model to describe the role of the TUTT in early season typhoon development in the western Pacific near the equatorial monsoon trough. He suggested that a TUTT might have three effects on TC development. First, the accompanying subequatorial ridge on the south side of a TUTT lies over the low-level low that may decrease the vertical shear; second, a divergent flow on the south and east sides of the cyclonic circulation in a TUTT may increase the ventilation aloft to help in the development of a low-level low; and third, a channel to large-scale westerlies may be established for the efficient outflow of the heat released by the increased convection in the developing depression.

Based on these previous studies, we found 3 out of the 10 remaining cases may be associated with the upper-tropospheric forcing. An example is Typhoon Nari, which formed on 6 September 2001 (Fig. 11). Two days prior to its formation, an upper-level trough was located approximately 20° longitude west of the genesis location. One day later, this trough moved 10° longitude eastward. In the mean time, this upper-level trough deepened, and the southwesterly flow on the eastern side of the trough became stronger. On the day Nari formed, this trough was less than 5° to the northwest of Nari's genesis position. As a result, strong southwesterlies dominated in this area, and an outflow channel was set up in the upper levels north of Nari. This led to the enhancement of low-level disturbances and may be responsible for Nari's genesis.

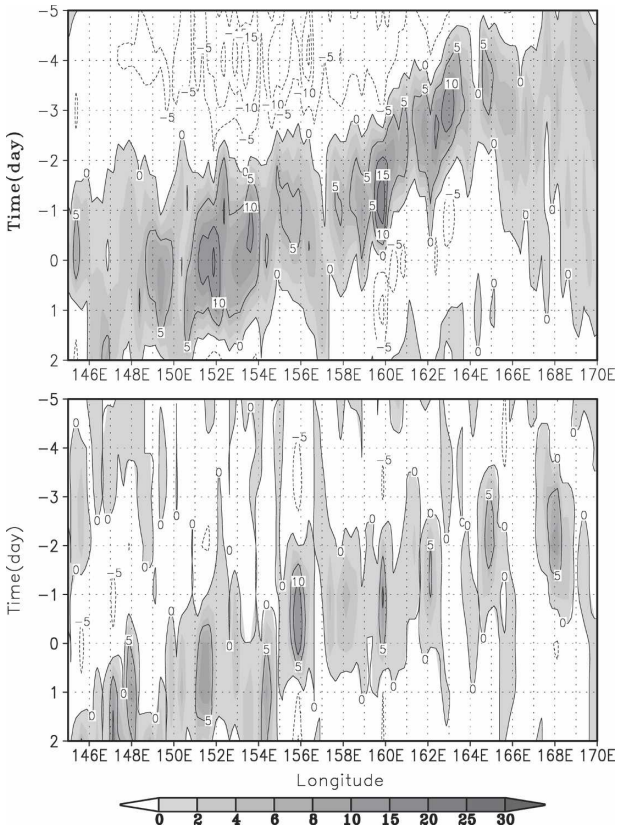

FIG. 8. Time–longitude profiles of (top) the TMI surface perturbation kinetic energy $(u^2 + v^2)'/2$ ($m^2 s^{-2}$) and (bottom) precipitation rate (mm day^{-1}) along 25°N. The horizontal axis is longitude and the vertical axis is time in days. Typhoon Kong-rey formed at 25°N, 150.2°E on 22 Jul 2001 (corresponding to day 0). Both panels show clear westward-propagating signals prior to the birth of Kong-rey.

2) TC GENESIS TO THE WEST OF A PREVIOUS TC

For the TCED scenario, a new TC may form to the east (in the wake) of a preexisting TC. However, we noticed a few cases in which a new TC formed to the west of a preexisting TC. There are 4 such cases among the 10 remaining cases. The similarities among these four cases suggest that they may share the same formation characteristics. For example, they all formed in or near the South China Sea (SCS), they formed on the day when the preexisting TCs moved northwestward and passed the latitude of the new genesis, and they formed when the distance between the old and new TCs was within 1500–2000 km.

Figure 12 shows the formation of Typhoon Kai-tak on 5 July 2000, which was categorized into this type. Two days prior to the formation of Kai-tak (solid dot), a mature TC, Kirogi (marked with an A), was located to the southeast of this genesis point. The easterly flows north of Kirogi can be clearly seen (on 3 July 2000). Meanwhile, a weak cyclonic circulation can be seen off the western coastline of Luzon Island. One day later, Kirogi reached the latitude where Kai-tak formed. The continuous (2 day) low-level convergence between the prevailing southwesterlies and Kirogi's northeasterlies enhanced the cyclonic vorticity of the cyclonic system and finally led to the genesis of Kai-tak at 19.1°N and 120.2°E.

We speculate that this type of TC genesis may be common in the WNP. Physical mechanisms associated with this type of cyclogenesis require further study. One possible mechanism may be the interaction between a prior TC and the monsoon flow, as in the Kai-tak case. When a mature TC moves northward, the low-level northeasterlies to the northwest of the cyclone can interact with the mean prevailing southwesterlies in the SCS to form/enhance the low-level convergence and cyclonic vorticity that finally leads to TC genesis.

3) CYCLOGENESIS ASSOCIATED WITH PREEXISTING CONVECTIVE ACTIVITIES

It has been noted that some TC genesis events were associated with preexisting convective activities but without a clear surface cyclonic flow. An example is given in Fig. 13 for Typhoon Usagi, which formed on 9 August 2001. Three days prior to the genesis of Usagi, intense convection had already appeared over the region where the storm formed. However, from the 3–8-day filtered QuikSCAT wind fields, there was no significant cyclonic wind perturbation. A clear cyclonic circulation appeared in the wind fields only 1 day prior to the TC genesis. Several possible mechanisms may be responsible for this type of TC formation. For one, cyclonic circulation may first develop at the midlevel and then extend downward to the surface. This midlevel initiation process has been previously suggested by Simpson et al. (1997) and Bister and Emanuel (1997). Another possible mechanism is related to the "hot tower" concept where randomly distributed convective disturbances may be organized into a well-defined vortex through a merger and axisymmetrization (Hendricks et al. 2004). Numerical simulations with high resolutions are needed for future assessments.

4. Intraseasonal modulation of the WNP cyclogenesis

In addition to having a significant annual cycle, TC genesis also experiences a strong subseasonal variation. It has been suggested that the variability of TC occurrence is modulated by low-frequency atmospheric vari-

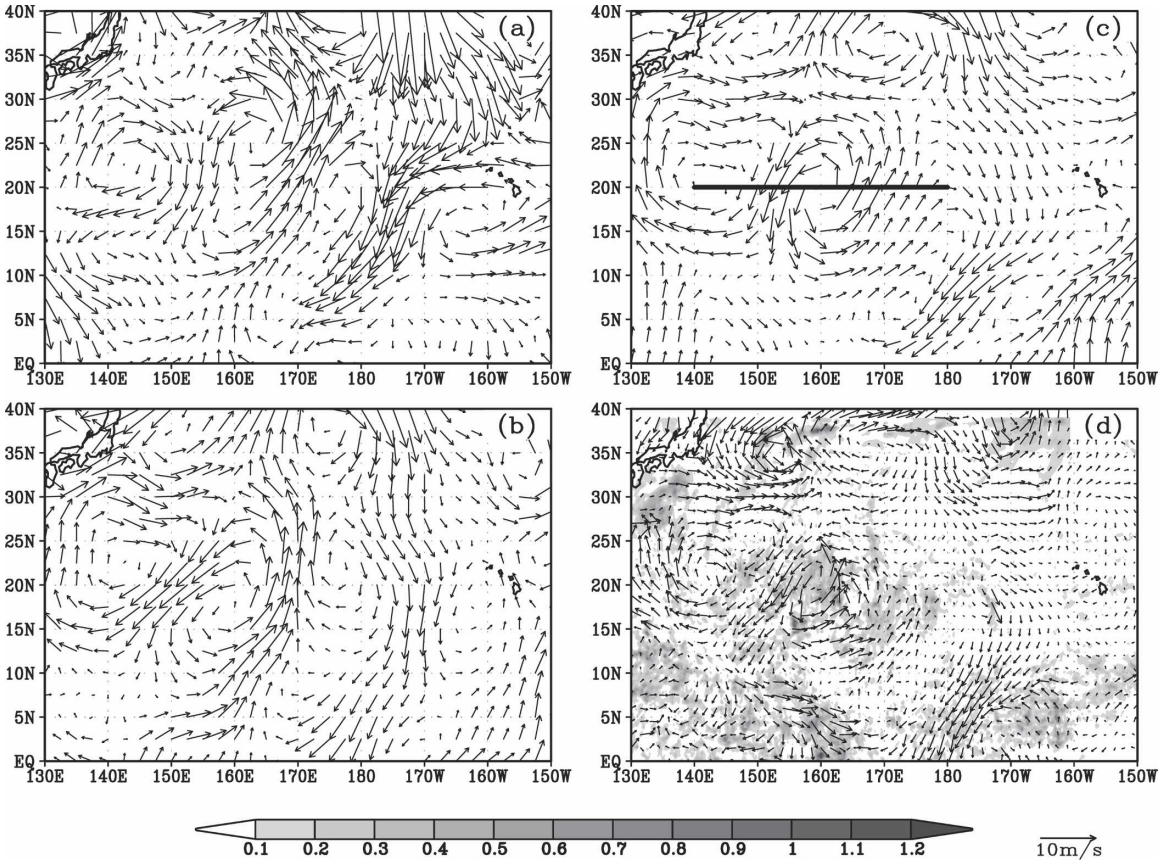

FIG. 9. Horizontal structure of the observed easterly wave on 18 Jul 2001. The wind fields are 3–8-day filtered NCEP–NCAR reanalysis data at (a) 200, (b) 400, and (c) 600 hPa. (d) The 3–8-day filtered QuikSCAT surface wind and TMI cloud liquid water data (shading; mm).

ability associated with the tropical ISO (Gray 1979). Recent observational studies have confirmed the close relationship between TC genesis and the ISO (Yamazaki and Murakami 1989; Hartmann et al. 1992; Liebmann et al. 1994; Maloney and Hartmann 2000). Several studies have theoretically addressed how the ISO modulates TC activities (Maloney and Hartmann 2001; Sobel and Maloney 2000; Maloney and Dickinson 2003). Maloney and Dickinson (2003) indicated that the modulation is a result of enhancing or suppressing the TD-type disturbances in the lower troposphere. The enhancement of the TD-type disturbances is attributed either to Rossby wave accumulation caused by large-scale convergence (Holland 1995; Sobel and Bretherton 1999) or through a barotropic conversion during ISO westerly phases (Sobel and Maloney 2000; Maloney and Dickinson 2003). Kuo et al. (2001) argued that the enhanced westerlies ahead of the Madden–Julian oscillation and the background easterlies also provide a favorable basic state for the nonlinear wave accumulation and scale contraction for the energy dispersion mechanism.

Here, we have evaluated the impacts of the ISO on TC formation in the WNP for the 2000 and 2001 summer seasons. The pattern and the characteristics of the ISO are represented by the 20–70-day filtered OLR and 850-hPa zonal wind fields. There are two reasons for selecting these two variables. First, they are independent of each other in terms of data sources. Second, they have been widely used to represent ISO activity in many previous studies. Observational studies show that the ISO is characterized by enhanced (suppressed) convection and westerly (easterly) 850-hPa zonal winds in its active (suppressed) phase. From a thermodynamic prospective, enhanced convection provides a greater large-scale low-level moisture convergence that favors the development of tropical depressions. From a dynamic perspective, the ISO westerly anomaly helps to increase the cyclonic vorticity to the north and creates a favorable environment for tropical depression development. Therefore, more TCs may form in the active phase of the ISO.

We compute time series of area-averaged (5°–25°N, 110°–160°E) OLR perturbations. The results are shown

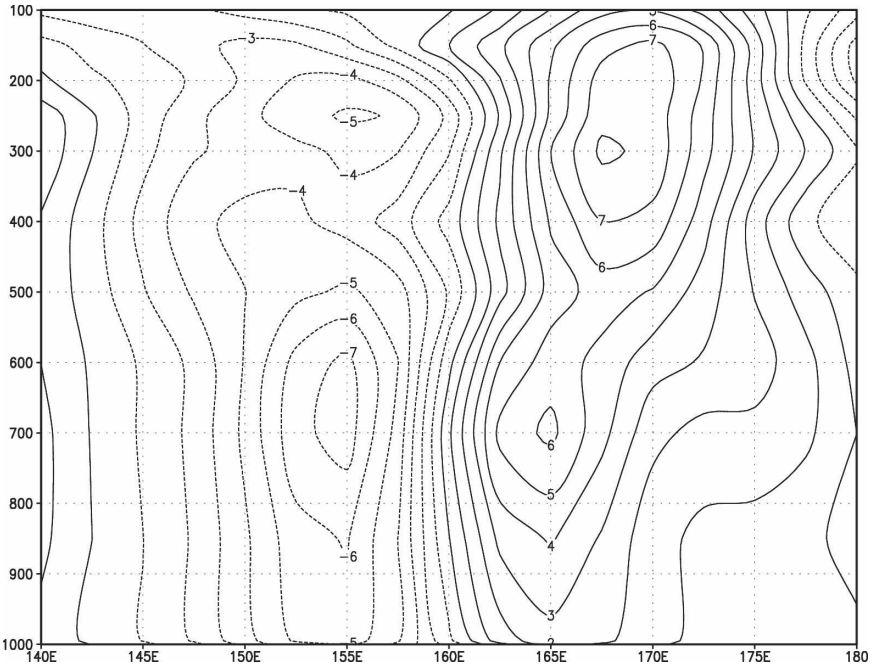

FIG. 10. Cross section of NCEP–NCAR reanalysis meridional wind perturbations along 20°N as shown in Fig. 9. Vertical axis indicates pressure levels from 1000 to 100 hPa.

as the curves in the left panels of Fig. 14. According to this OLR variation, there are two major active-phase (negative OLR perturbations) ISO events in the WNP each year (i.e., from 28 June to 15 July and from 6 August to 5 September 2000, and from 16 June to 6 July and from 8 to 26 August 2001). Figure 14 also shows the area-averaged OLR and zonal wind perturbations for those 34 genesis cases in 2000 and 2001. For the OLR perturbations, we selected a 5° × 5° box centered at the TC genesis location. For the zonal wind perturbations, the selected 5° × 5° box is to the south of the TC genesis position. It appears that TC activities in both years are, to a certain extent, influenced by the active phase of the ISO, especially in 2000.

Horizontal composites are made for the 20–70-day filtered OLR and the 850-hPa zonal wind fields centered on the TCs (Fig. 15). The cyclogenesis events are associated with the minimum OLR perturbations (enhanced convection) and the westerly perturbations to the south of the TC genesis region. This figure further supports the notion that the TC formations were significantly modulated by the ISO activities in 2000 and 2001.

5. Summary and discussion

High-resolution satellite (QuikSCAT and TMI) and NCEP–NCAR reanalysis data are used to analyze 34 cyclogenesis events in the WNP during the 2000 and 2001 typhoon seasons. Three types of synoptic-scale disturbances (TCEDs, SWTs, and EWs) are identified from the near-surface data as the major pregenesis features, each associated with a different mechanism. Among these 34 cyclogenesis cases, 6 are associated with TCEDs, 11 are associated with SWTs, and 7 are associated with EWs. They account for 71% of the total TC genesis events during these two years.

While a TC moves northwestward, Rossby waves emit energy southeastward. As a result, a synoptic-scale Rossby wave train with alternating anticyclonic and cyclonic vorticity perturbations forms in its wake. Our analyses indicate that not all TCs produce Rossby wave trains at their wakes. Stronger TCs in a weaker background flow are more likely to produce a Rossby wave train. New TCs are observed to form in the cyclonic vorticity region of the wave train. However, not all TC-related Rossby wave trains eventually lead to the formation of a new TC. The large-scale environmental flow plays an important role in determining whether a cyclonic circulation in a wave train can develop into a new TC. The second type of precursors is a SWT that is not associated with a preexisting storm. Mechanisms for the TC formation associated with this wave train are similar to those linked to TC dispersive waves. In more detail, some of the SWTs are related to equatorial MRG waves. The evolutionary characteristics of EWs

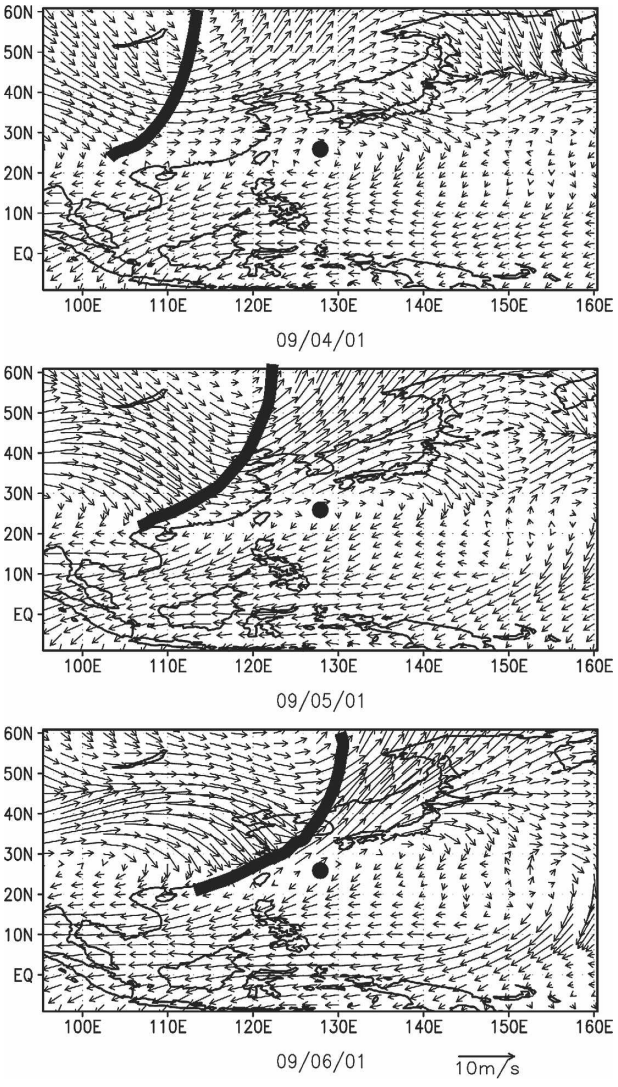

FIG. 11. NCEP–NCAR reanalysis 200-hPa wind evolution prior to the formation of Typhoon Nari. The dots represent the genesis location of Nari on 6 Sep 2001. The thick solid curve in each panel represents the trough.

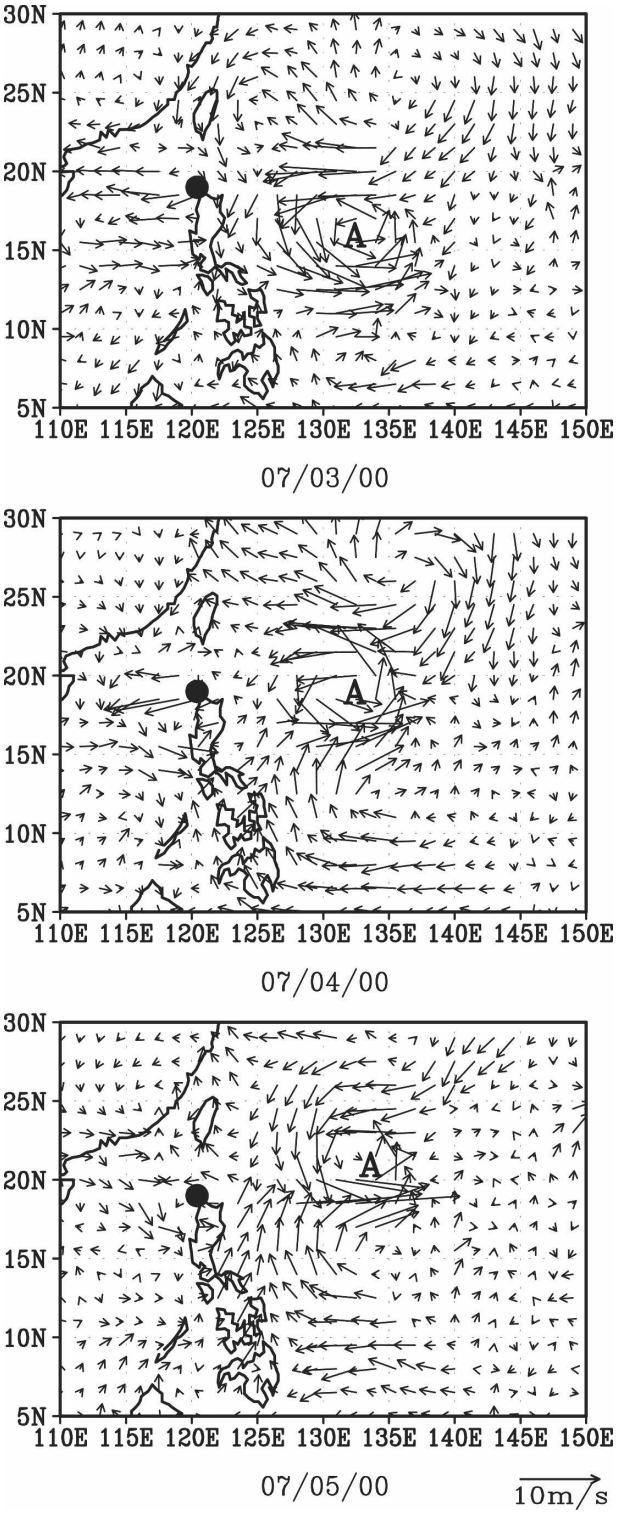

FIG. 12. Time evolution of QuikSCAT 3–8-day filtered surface winds prior to the formation of Typhoon Kai-tak, which formed on 5 Jul 2000. The letter A denotes the preexisting Typhoon Kirogi. The dots represent the location where Kai-tak formed.

reveal a zonal scale contraction characteristic prior to the cyclogenesis.

While we present pregenesis disturbances that evolve into TCs, the formation of the cyclones requires mechanisms mostly associated with environmental forcing. Kuo et al. (2001) demonstrated that a northwestward propagation pattern with an approximately 8-day period and 3000-km wavelength could be produced by the energy dispersion of the intensified disturbance under a confluent, opposite mean flow. The intensified disturbance may disperse energy upstream, leading to a series of trailing anticyclonic and cyclonic cells along the northwestward propagation path. When the background scale contraction is present, the energy disper-

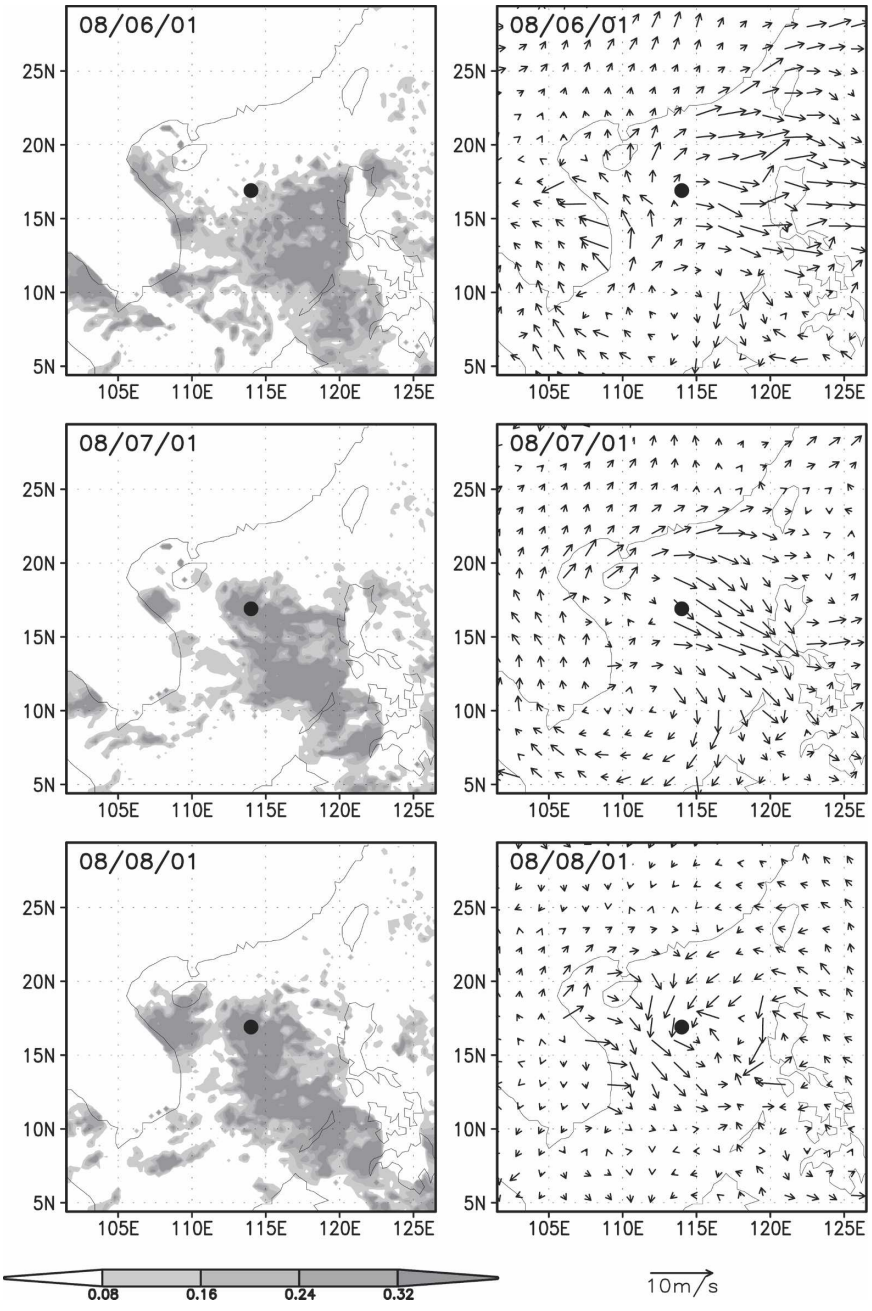

FIG. 13. Time evolution of (left) TMI cloud liquid water and (right) 3–8-day filtered QuikSCAT surface wind prior to the genesis of TC Usagi, which formed on 9 Aug 2001. The dots indicate the location where Usagi formed.

sion leads to the formation of new disturbances by the axisymmetrization dynamics. Tropical cyclone genesis often clusters along the confluent zone and the SWT path. It appears that the energy dispersion and the scale contraction mechanism may also contribute to the SWT and EW groups if there is a preintensified disturbance. Thus, it is likely that scale contraction and energy accumulation, as proposed by Kuo et al. (2001), may be the major mechanisms for all three types of prestorm disturbances.

Further examinations of upper-tropospheric signals and preexisting convective activity conditions suggest three additional genesis scenarios. The first one is associated with the upper-level trough forcing, the second one is the formation to the west of a preexisting TC with its wind interacting with the monsoon mean south-

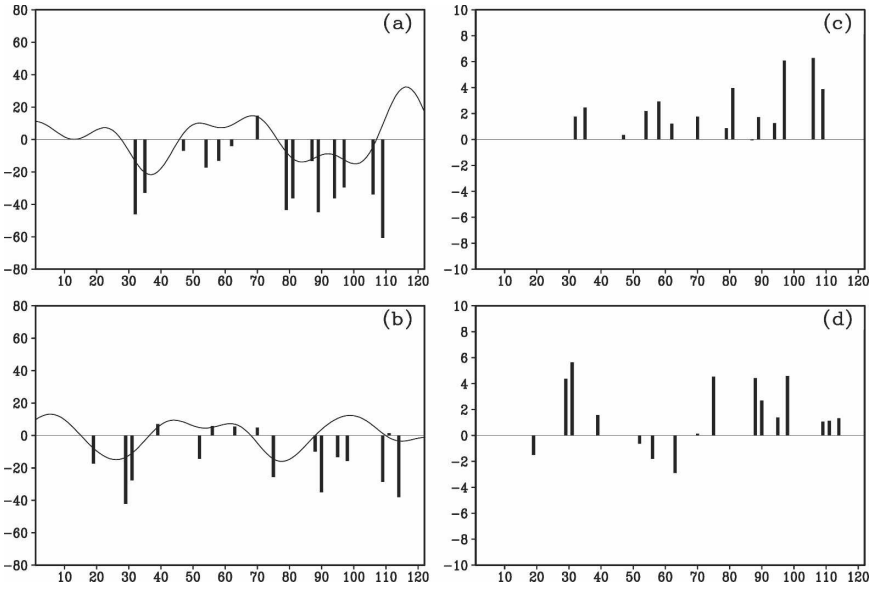

FIG. 14. (left) The 20–70-day filtered NCEP–NCAR OLR (W m^{-2}) and (right) the 850-hPa zonal wind (m s^{-1}) in (top) 2000 and (bottom) 2001 as a function of time (from 1 Jun to 30 Sep, totaling 122 days). Each bar represents the (left) OLR perturbations at the location of TC genesis when TCs occur or (right) the 850-hPa zonal wind perturbations to the south of the TC genesis center. The curves in the left panels are time series of the 20–70-day filtered OLR averaged in the domain 5°–25°N, 110°–160°E). [Note that for the special cases when two TCs formed on the same day (5 Sep 2000, 22 Jul 2001, and 27 August 2001), the bars here represent the averaged values of the filtered OLR or 850-hPa zonal winds.]

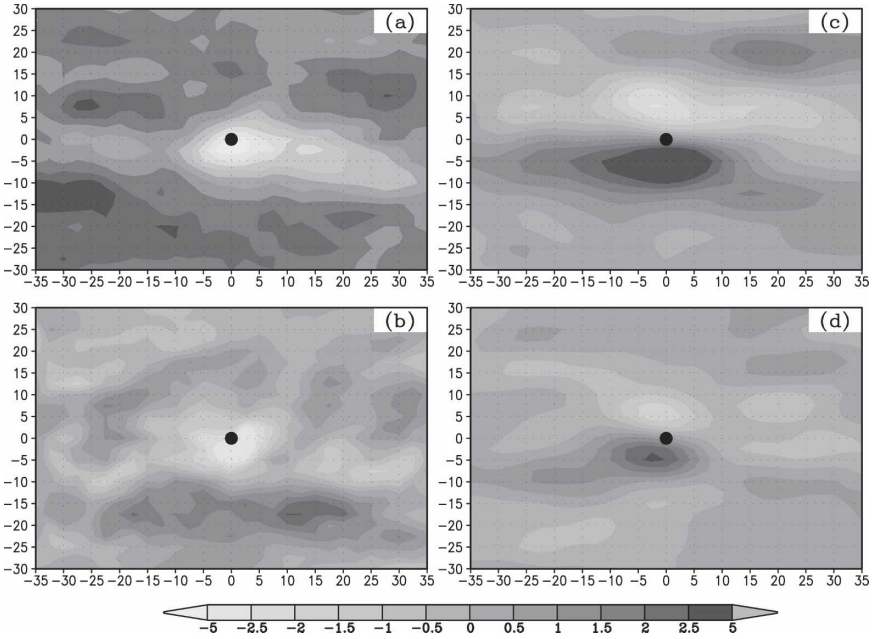

FIG. 15. Horizontal composites of the 20–70-day filtered NCEP–NCAR OLR and 850-hPa zonal wind data. The vertical (horizontal) axis is relative distance in degrees latitude (longitude) to the composite TC center (marked as dots): (a) OLR in 2000, (b) OLR in 2001, (c) 850-hPa zonal wind in 2000, and (d) 850-hPa zonal wind in 2001 (units for OLR, ×5 W m^{-2}; units for wind, m s^{-1}).

westerly flow, and the third type has vigorous convective activities with no significant surface flow signatures. Model simulations are needed to examine in detail these special genesis scenarios, and these experiments are beyond the scope of this study.

Our analysis also shows a close relationship between the ISO and the TC genesis events. Through a composite analysis of OLR and zonal wind perturbations, we found that TC formation was significantly modulated by the ISO activities in both 2000 and 2001.

The satellite data analysis provides observational evidence of how the disturbances associated with TCEDs, SWTs, and EWs evolve prior to tropical cyclogenesis. It is likely that in reality TC genesis in the aforementioned scenarios may involve more than one of the scenarios mentioned above, for example, both the EW and upper-tropospheric forcing scenarios. This study highlights the importance of the TCEDs, SWTs, and EWs as precursors to the TC formation. Therefore, the challenge in the numerical prediction of tropical cyclogenesis depends critically on accurate signals of the synoptic waves/perturbations in the initial state. The new satellite-derived products (such as the Advanced Microwave Sounding Units) have been proven to be successful in providing the three-dimensional spatial structure and temporal evolution of atmospheric temperature and moisture fields over the oceans (Zhu et al. 2002). These products, together with other available data such as the QuikSCAT and TMI products, will provide detailed tropical wave structures. By properly assimilating these data into numerical models to represent the initial wave structures, one may expect success in predicting TC genesis events.

Acknowledgments. The authors thank the anonymous reviewers for their constructive comments and suggestions. We thank Drs. Bin Wang and Yuqing Wang for valuable discussions. The first two authors were supported by NRL Subcontract N00173-06-1-G031 and ONR Grants N00014-021-0532 and N00014-031-0739. The third author was supported in part by the Naval Research Laboratory and the Office of Naval Research under Program Element 62435N, Project BE-435-003. The International Pacific Center is partially sponsored by the Japan Agency for Marine–Earth Science and Technology (JAMSTEC).

REFERENCES

Anthes, R. A., 1982: *Tropical Cyclones: Their Evolution, Structure and Effects. Meteor. Mongr.,* No. 41, Amer. Meteor. Soc., 208 pp.

Bister, M., and K. A. Emanuel, 1997: The genesis of Hurricane Guillermo: TEXMEX analyses and a modeling study. *Mon. Wea. Rev.,* **125,** 2662–2682.

Briegel, L. M., and W. M. Frank, 1997: Large-scale influences on tropical cyclogenesis in the western North Pacific. *Mon. Wea. Rev.,* **125,** 1397–1413.

Carr, L. E., III, and R. L. Elsberry, 1994: Systematic and integrated approach to tropical cyclone track forecasting. Part I. Approach overview and description of meteorological basis. NPS Tech. Rep. NPS-MR-94-002, 273 pp.

——, and ——, 1995: Monsoonal interactions leading to sudden tropical cyclone track changes. *Mon. Wea. Rev.,* **123,** 265–289.

Chang, C.-P., V. F. Morris, and J. M. Wallace, 1970: A statistical study of easterly waves in the western Pacific: July–December 1964. *J. Atmos. Sci.,* **27,** 195–201.

——, J.-M. Chen, P. A. Harr, and L. E. Carr, 1996: Northwestward-propagating wave patterns over the tropical western North Pacific during summer. *Mon. Wea. Rev.,* **124,** 2245–2266.

Colon, J. A., and W. R. Nightingale, 1963: Development of tropical cyclones in relation to circulation patterns at the 200 millibar level. *Mon. Wea. Rev.,* **91,** 329–336.

Davidson, N. E., and H. H. Hendon, 1989: Downstream development in the Southern Hemisphere monsoon during FGGE/WMONEX. *Mon. Wea. Rev.,* **117,** 1458–1470.

Dickinson, M., and J. Molinari, 2002: Mixed Rossby–gravity waves and western Pacific tropical cyclogenesis. Part I: Synoptic evolution. *J. Atmos. Sci.,* **59,** 2183–2196.

Flierl, G. R., 1984: Rossby wave radiation from a strongly nonlinear warm eddy. *J. Phys. Oceanogr.,* **14,** 47–58.

——, and K. Haines, 1994: The decay of modons due to Rossby wave radiation. *Phys. Fluids,* **6,** 3487–3497.

——, M. E. Stern, and J. A. Whitehead Jr., 1983: The physical significance of modons: Laboratory experiments and general integral constrains. *Dyn. Atmos. Oceans,* **7,** 233–263.

Frank, W. M., 1982: Large-scale characteristics of tropical cyclones. *Mon. Wea. Rev.,* **110,** 572–586.

Gray, W. M., 1968: Global view of the origin of tropical disturbances and storms. *Mon. Wea. Rev.,* **96,** 669–700.

——, 1975: Tropical cyclone genesis. Dept. of Atmospheric Science Paper 232, Colorado State University, Fort Collins, CO, 121 pp.

——, 1979: Hurricanes: Their formation, structure, and likely role in the tropical circulation. *Meteorology over the Tropical Oceans,* D. B. Shaw, Ed., Royal Meteorological Society, 155–218.

Hartmann, D. L., M. L. Michelsen, and S. A. Klein, 1992: Seasonal variations of tropical intraseasonal oscillations: A 20–25-day oscillation in the western Pacific. *J. Atmos. Sci.,* **49,** 1277–1289.

Hendricks, E. A., M. T. Montgomery, and C. A. Davis, 2004: The role of vertical hot towers in the formation of Tropical Cyclone Diana (1984). *J. Atmos. Sci.,* **61,** 1209–1232.

Holland, G. J., 1995: Scale interaction in the western Pacific monsoon. *Meteor. Atmos. Phys.,* **56,** 57–79.

Kuo, H.-C., J.-H. Chen, R. T. Williams, and C.-P. Chang, 2001: Rossby waves in zonally opposing mean flow: Behavior in northwest Pacific summer monsoon. *J. Atmos. Sci.,* **58,** 1035–1050.

Lau, K.-H., and N.-C. Lau, 1990: Observed structure and propagation characteristics of tropical summertime synoptic-scale disturbances. *Mon. Wea. Rev.,* **118,** 1888–1913.

——, and ——, 1992: The energetics and propagation dynamics of tropical summertime synoptic-scale disturbances. *Mon. Wea. Rev.,* **120,** 2523–2539.

Li, T., 2006: Origin of the summertime synoptic-scale wave train in the western North Pacific. *J. Atmos. Sci.,* **63,** 1093–1102.

——, and B. Fu, 2006: Tropical cyclogenesis associated with Rossby wave energy dispersion of a preexisting typhoon. Part I: Satellite data analyses. *J. Atmos. Sci.,* **63,** 1377–1389.

——, ——, X. Ge, B. Wang, and M. Peng, 2003: Satellite data analysis and numerical simulation of tropical cyclone formation. *Geophys. Res. Lett.,* **30,** 2122–2126.

Liebmann, H., H. Hendon, and J. D. Glick, 1994: The relationship between tropical cyclones of the western Pacific and Indian Oceans and the Madden–Julian oscillation. *J. Meteor. Soc. Japan,* **72,** 401–411.

Luo, Z., 1994: Effect of energy dispersion on the structure and motion of tropical cyclone. *Acta Meteor. Sin.,* **8,** 51–59.

Maloney, E. D., and D. L. Hartmann, 2000: Modulation of eastern North Pacific hurricanes by the Madden–Julian oscillation. *J. Climate,* **13,** 1451–1460.

——, and ——, 2001: The Madden–Julian oscillation, barotropic dynamics, and North Pacific tropical cyclone formation. Part I: Observations. *J. Atmos. Sci.,* **58,** 2545–2558.

——, and M. J. Dickinson, 2003: The intraseasonal oscillation and the energetics of summertime tropical western North Pacific synoptic-scale disturbances. *J. Atmos. Sci.,* **60,** 2153–2168.

McBride, J. L., and R. Zehr, 1981: Observational analysis of tropical cyclone formation. Part II: Comparison of non-developing versus developing systems. *J. Atmos. Sci.,* **38,** 1132–1151.

McDonald, N. R., 1998: The decay of cyclonic eddies by Rossby wave radiation. *J. Fluid Mech.,* **361,** 237–252.

Murakami, M., 1979: Large-scale aspects of deep convective activity over the GATE area. *Mon. Wea. Rev.,* **107,** 994–1013.

Reed, R. J., and E. E. Recker, 1971: Structure and properties of synoptic-scale wave disturbances in the equatorial western Pacific. *J. Atmos. Sci.,* **28,** 1117–1133.

——, D. C. Norquist, and E. E. Recker, 1977: The structure and properties of African wave disturbances as observed during phase III of GATE. *Mon. Wea. Rev.,* **105,** 317–333.

Riehl, H., 1948: On the formation of typhoons. *J. Meteor.,* **5,** 247–264.

Ritchie, E. A., and G. J. Holland, 1997: Scale interactions during the formation of Typhoon Irving. *Mon. Wea. Rev.,* **125,** 1377–1396.

——, and ——, 1999: Large-scale patterns associated with tropical cyclogenesis in the western Pacific. *Mon. Wea. Rev.,* **127,** 2027–2043.

Sadler, J. C., 1976: A role of the tropical upper tropospheric trough in early season typhoon development. *Mon. Wea. Rev.,* **104,** 1266–1278.

Shapiro, L. J., 1977: Tropical storm formation from easterly waves: A criterion for development. *J. Atmos. Sci.,* **34,** 1007–1021.

——, and K. V. Ooyama, 1990: Vortex evolution on a beta plane. *J. Atmos. Sci.,* **47,** 170–187.

Simpson, J., E. Ritchie, G. J. Holland, J. Halverson, and S. Stewart, 1997: Mesoscale interactions in tropical cyclone genesis. *Mon. Wea. Rev.,* **125,** 2643–2661.

Sobel, A. H., and C. S. Bretherton, 1999: Development of synoptic-scale disturbances over the summertime tropical northwest Pacific. *J. Atmos. Sci.,* **56,** 3106–3127.

——, and E. D. Maloney, 2000: Effect of ENSO and ISO on tropical depressions. *Geophys. Res. Lett.,* **27,** 1739–1742.

Takayabu, Y. N., and T. Nitta, 1993: 3–5-day period disturbances coupled with convection over the tropical Pacific Ocean. *J. Meteor. Soc. Japan,* **71,** 221–245.

Webster, P. J., and H.-R. Chang, 1988: Equatorial energy accumulation and emanation regions: Impacts of a zonally varying basic state. *J. Atmos. Sci.,* **45,** 803–829.

Yamazaki, N., and M. Murakami, 1989: An intraseasonal amplitude modulation of the short-term tropical disturbances over the western Pacific. *J. Meteor. Soc. Japan,* **67,** 791–807.

Yanai, M., 1961: A detailed analysis of typhoon formation. *J. Meteor. Soc. Japan,* **39,** 187–214.

——, T. Maruyama, T. Nitta, and Y. Hayashi, 1968: Power spectra of large-scale disturbances over the tropical Pacific. *J. Meteor. Soc. Japan,* **46,** 308–323.

Zhu, T., D.-L. Zhang, and F. Weng, 2002: Impact of the Advanced Microwave Sounding Unit measurements on hurricane prediction. *Mon. Wea. Rev.,* **130,** 2416–2432.